crust and upper mantle. *J. Geophys. Res*., 2006, **111**, B10301, doi:10.1029/2005JB004062.
11. Waldhauser, F., hypoDD – A program to compute double-difference hypocenter locations. US Geological Survey open-file report 01-113, 2001, p. 113.
12. de la Torre, T. L., Monsalve, G., Sheehan, A. F., Sapkota, S. and Wu, F., Earthquake processes of the Himalayan collision zone in eastern Nepal and the southern Tibetan Plateau. *Geophys. J. Int*., 2007, **171**, 718–738.
13. Burov, E. B. and Watts, A. B., The long-term strength of continental lithosphere: 'jelly sandwich' or 'crème-brûlée'? *GSA Today*, 2006, **16**, 4–10; doi:10.1130/1052-5173.
14. Nath, S. K., Thingbaijam, K. K. S. and Ghosh, S. K., Earthquake catalogue of South Asia – a generic MW scale framework. 2010; www.earthqhaz.net/sacat.
15. http://www.globalcmt.org/CMTsearch.html

ACKNOWLEDGEMENTS. We thank Dr Y. J. Bhaskar Rao, Director, NGRI, Hyderabad for support and releasing funds necessary for the installation and operation of seismic stations. Part of the work has been performed under the project supported by the Ministry of Earth Sciences, Government of India. We thank Dr H. V. Satyanarayana for sparing a broadband sensor and logger, and N. Purnachandra Rao for discussions.

Received 22 December 2011; accepted 27 January 2012

Triggering of aftershocks of the Japan 2011 earthquake by Earth tides

A. Datta and Kamal*

Department of Earth Sciences, Indian Institute of Technology, Roorkee 247 667, India

The aftershock sequence of the devastating Japan earthquake of March 2011 is analysed for the presence of periodicities at the Earth tide periods. We use spectral analysis as well as a time-domain method, KORRECT, developed earlier to detect the presence of diurnal and semi-diurnal periodicities in the sequence of aftershocks ($M \geq 4$). This suggests that large aftershocks in the fault zone of the Japan 2011 earthquake were strongly influenced by Earth tides.

Keywords: Aftershock triggering, Earth tides, Japan 2011 earthquake, spectral analysis.

THE elastic rebound theory is now well accepted as the reason for the occurrence of earthquakes. When fault stresses rise above a critical threshold for rupture[1], the Earth slips along the fault and an earthquake results. It is then only intuitive that any additional stress acting on a fault system that approaches failure could trigger the rupture process that produces the earthquake. The stresses responsible for the occurrence of an earthquake are tectonic in origin, but the final onset of rupture can be affected by other kinds of stresses superimposed on tectonic stresses during the build-up to failure. We use the term 'affected' here because the additional stress may advance or retard the onset of rupture, depending on the sense in which it acts.

Perhaps the strongest candidate for earthquake triggering is the Earth tide. Gravitational attractions, primarily of the sun and moon, cause periodic elastic deformation of the solid Earth, thus exerting additional stresses. These tidal stresses are oscillatory in nature and their magnitude is of the order of 10^3 Pa. This is much less than average stress drops in earthquakes[2] (10^5–10^7 Pa), but the rate of tidal stress change is much higher than the build-up rate of tectonic stress[3] rate, and this makes tidal triggering of earthquakes possible.

The question of whether earthquakes are triggered by Earth tides was raised over a century ago[4,5] and since then, numerous efforts have been directed towards answering it. These studies investigated different kinds of datasets and employed a variety of methods[6], but owing to mixed results[2,7–10], no conclusive evidence had emerged until recently for earthquake triggering by the Earth tides. In the last decade, tests on tidal triggering have produced more homogeneous and positive results. A breakthrough was achieved recently[11] when the triggering effect of the earth tide was demonstrated in earthquakes of all magnitudes (> 2.5) and all types of focal mechanisms, using the largest global earthquake catalogue (NEIC world seismic catalogue) available. In 2004, a study of seismicity in Japan[12] found that regions which experienced a large earthquake showed the best earthquake–tide correlations. These two findings were the motivation for our search for tidal triggering of aftershocks of the recent earthquake in Japan. Additionally, an aftershock sequence is a type of dataset that is amenable to the simple methods of analysis employed in this study[13].

The Tohoku-Oki earthquake (magnitude $Mw = 9$) off the east coast of Honshu, Japan, occurred at 05:46:24.56 UT on 11 March 2011. The epicentre location was 38.299°N, 142.373°E and focal depth was 32 km. At the time of this study, an almost complete record of aftershocks of magnitude $Mw \geq 4$ occurring in the first 30 days following the main shock was available from the NEIC PDE catalogue of the US Geological Survey. Aftershock data obtained consisted of origin time, magnitude, epicentre location and focal depth. Since we are interested only in the events which occurred in the fault zone of the main shock, we have restricted this study to those events which occurred in the rectangular area between latitudes 34–41°N and longitudes 139.5–145.5°E. In this region, 1370 aftershocks (of $M \geq 4$) have been recorded by USGS in the one month following the main shock. These numbers make our dataset much larger than those used in previous studies of triggering of aftershocks[14–16]. We tested the completeness of the catalogue by linear least-squares fitting of the Guttenberg–

*For correspondence. (e-mail: kamal.iitr@gmail.com)

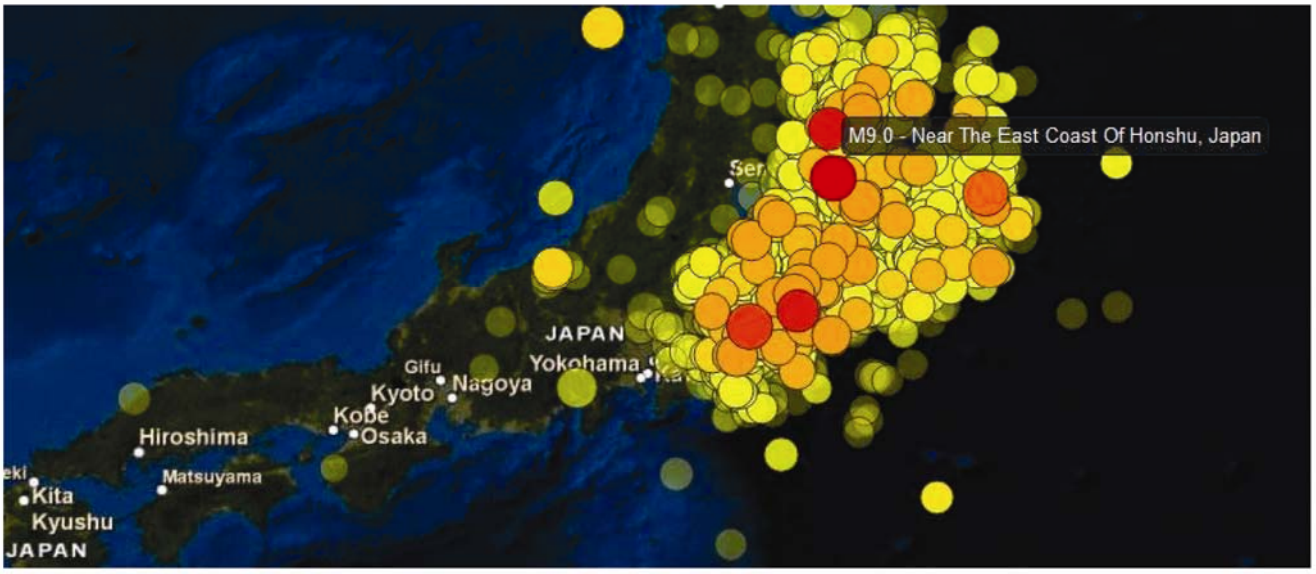

Figure 1. Distribution of Japan aftershocks. The colour scale represents time after the main shock, starting from red for 0, to green for 90 days after the main shock (increasing as red, orange, yellow, green). (Source: http://earthquake.usgs.gov/earthquakes/seqs/events/usc0001xgp/)

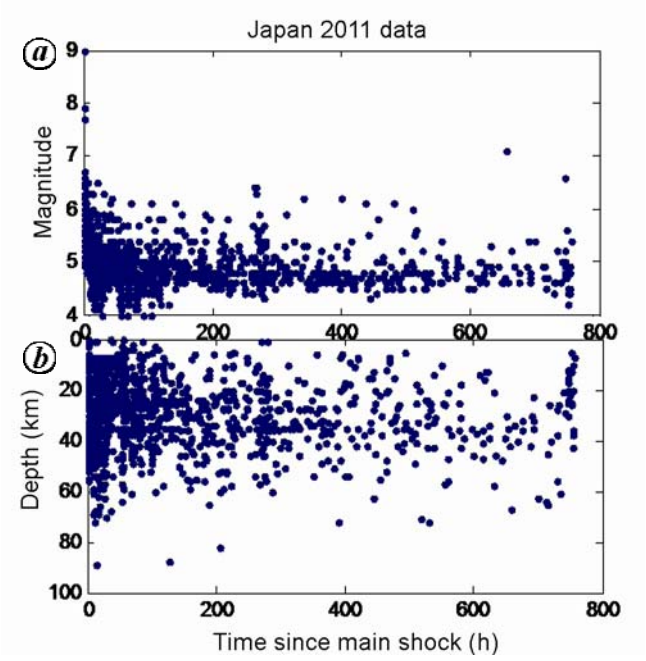

Figure 2. (***a***) Magnitude and (***b***) depth distributions of the entire Japan aftershock dataset during the first 30 days after the main shock.

Richter relation to the data and found a *b*-value of ~1.04, which is taken as acceptable. The spatial aftershock distribution is shown in Figure 1. Figure 2 shows the magnitude and depth distributions of aftershocks.

In this study, we first subjected the aftershock sequence to spectral analysis. Before this is done however, the sequence needs to be modified in order to obtain an equispaced time series with some meaningful amplitude. The time axis was divided into fixed width bins and the number of events in each bin was counted. This number was ascribed to the centre of the bin. The result was a time series with sampling interval equal to the bin width and amplitudes equal to the number of events per bin. Different bin widths, ranging from 20 min to 1 h were tried. All of these would allow the detection of frequencies several times higher than the strong tidal components. Each binned time series was tapered with a Tukey window and transformed to the frequency domain with the FFT routine in MATLAB.

The spectrum was computed for each of the binned series for the first 240 h (10 days) of data. Figure 3 shows the power spectra for two different values of bin width. The two distinct peaks are at 1 cycle per day and 1.9 cycles per day, corresponding to the diurnal and semi-diurnal components of the Earth tide. The same peaks were obtained in the spectra of all the binned series. However, this periodicity is not visible in the spectra of other sequences as shown in Figure 4.

The 240-h window was then shifted forward in time and the spectrum was computed for each window position. It was found that by the end of the 12th day after the main shock, it was impossible to detect any periodicities in the spectra. This is shown as a part of Figure 5 and is attributed to the sharp decline in the number of aftershocks with time. Our faith in the presence of tidal peaks in the power spectra was strengthened when we performed an identical analysis on the aftershock datasets from three other large earthquakes for which similar sized data were available from the same source – Indonesia 2004 (offshore Northern Sumatra, *Mw* 9.1), Indonesia 2005 (Northern Sumatra, *Mw* 8.6) and Chile 2010 (offshore Bio-Bio, *Mw* 8.8). These had 1361, 1253 and 1353 aftershocks respectively, in 30 days. Figure 4 shows the spectra obtained for a particular bin width; similar results

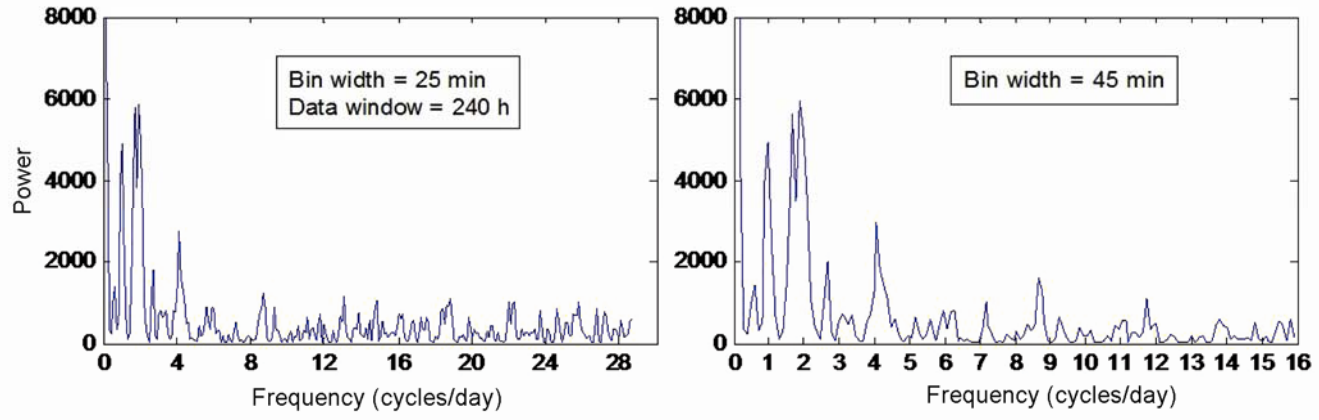

Figure 3. Power spectrum for two different binned series. The time series begins at the main shock and ends at 10 days after the main shock. In both cases, the peaks appear exactly at the same positions (1 and 1.9 cycles per day). Note the consistent nature of the peaks.

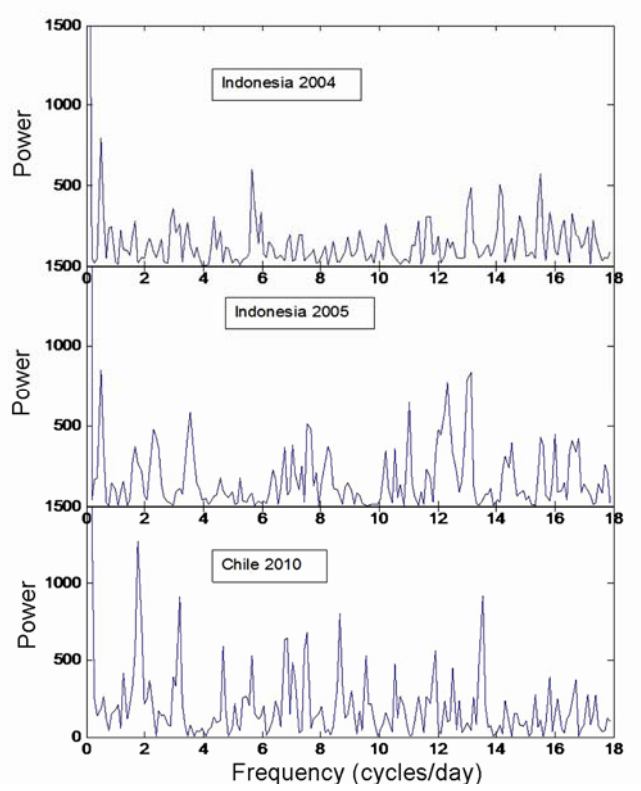

Figure 4. Power spectrum of aftershock sequences of three other $M > 8$ earthquakes. In each case the bin width was 40 min and the data used were from the first 240 h following the main shock. There are no peaks at tidal periods that rise above the background noise level in the signal, implying that tidal periodicities are not present in these sequences.

were obtained for other bin widths. Power spectra of series constructed from these datasets do not show any evidence for the presence of tidal periodicities and no account of tidal triggering of aftershocks of these earthquakes has ever been reported. The absence of tidal triggering in these sequences may be due to the fact that the Earth tide variation is a function of both space and time and it will only trigger under suitably favourable conditions.

Encouraged by the results of the spectral analysis, we employed a time-domain method known as KORRECT[13] to substantiate our results.

In this method, a pulse series is formed by repeating a finite-width rectangular pulse at regular intervals. The pulse width used here was the bin width used in the first method and the pulse separation, or the period of the pulse series, was made equal to the harmonic periods corresponding to the frequency samples obtained in the spectral analysis. This gives $N/2$ different periods for the pulse series, where N is the number of time samples used to compute FFT. For every such period, the pulse series was overlaid on the aftershock sequence in its original form. All the events falling within the pulses were counted and added up. This gave the number of aftershocks which had occurred at a particular phase of the period. On dividing this number by the total number of pulses that spanned the duration T of aftershock data, we obtained a measure of the aftershock 'density' (events per cycle) at a particular phase of the period. The pulse series was then shifted along the time axis, with pulse separation kept constant, to compute the aftershock density at another phase of the same period. We performed phase shifts in steps of 5°. A plot of the aftershock density as a function of phase gives the 'phase variation curve' for a particular period. If the phase variation curve for a particular period shows a significant rise/fall in aftershock density for certain phases, this indicates that in every cycle of an oscillating sequence with that period, anomalously high/low number of aftershocks is observed during that portion of the cycle. This clearly suggests triggering of aftershocks by that oscillating sequence. Most of the phase variation curves obtained in this analysis were not of this type. They were either flat or exhibited oscillatory behaviour around a mean value. However, when the period of the pulse series was made equal to

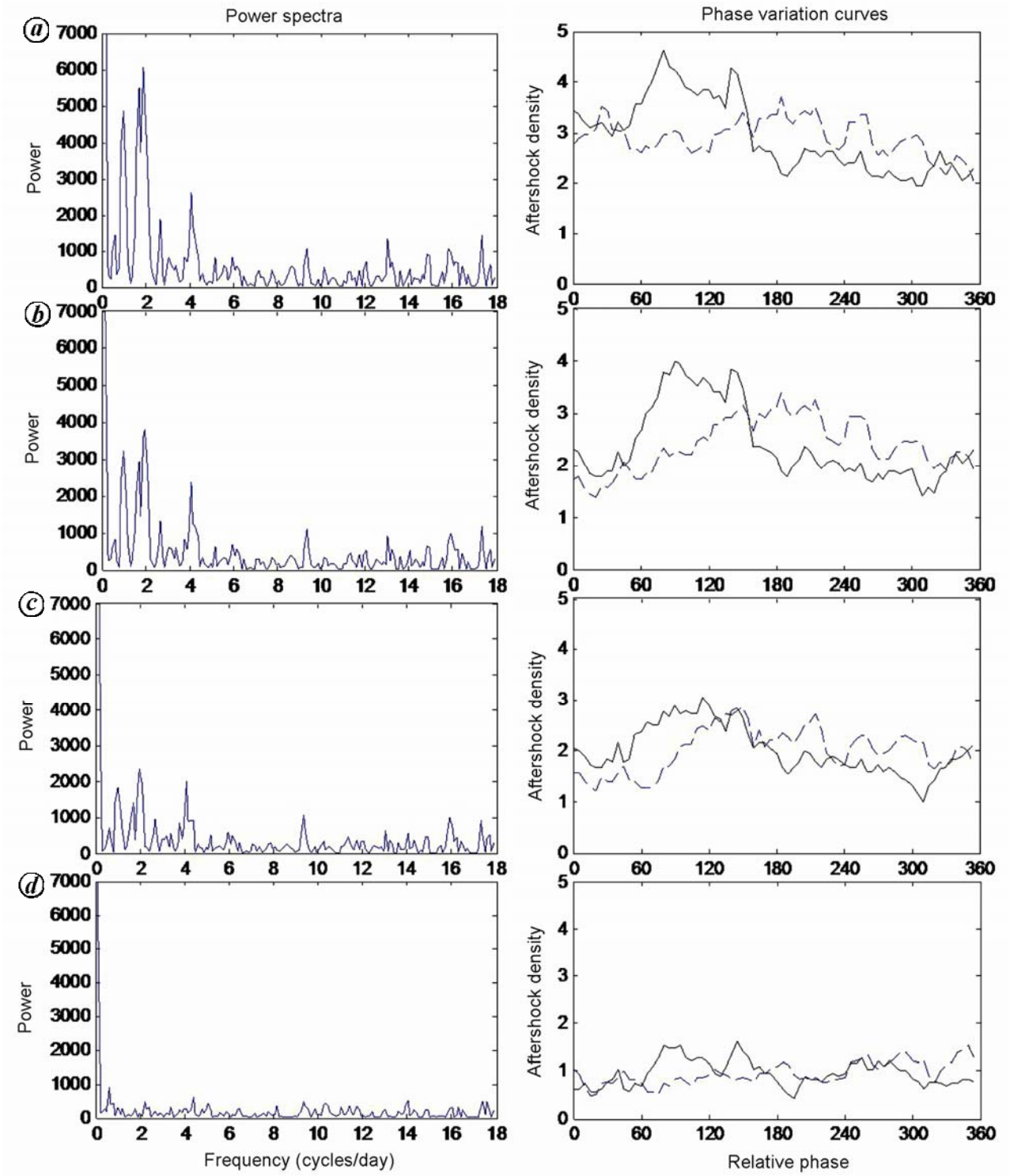

Figure 5. Comparison of frequency-domain (left panel) and time-domain (right panel) results for (***a***) 0 to 10 days, (***b***) 0.5 to 10.5 days, (***c***) 1 to 11 days and (***d***) 3 to 13 days after the main shock. Total length of data segment analysed in both domains is constant at 240 h. Phase plots have been obtained for 12.63 h and also 10.5 h (dashed line) for comparison. Bin width/pulse width is fixed at 40 min. In (***a***) and (***b***), note the trigger during the 60°–150° portion of the semi-diurnal tidal cycle. Also note that as the semi-diurnal spectral peak diminishes, its phase plot becomes increasingly unsystematic and similar to the phase plot for the 10.5 h period, which is not associated with any physical phenomenon.

the period corresponding to the frequencies at which peaks appear in the power spectra (periods of 12.63 h and 24 h), we obtained phase variation curves with a distinct character.

This can be seen in Figure 5 *a* and *b* for the 12.63 h period. Power spectra have also been shown in the left panel for comparison. It is clear from Figure 5 *a* and *b* that more aftershocks occur during a certain portion of

the semi-diurnal cycle, implying that certain phases of the cycle are favourable for the occurrence of aftershocks. This clearly suggests a trigger mechanism during this period. Similar phase plots were obtained for this period with different pulse widths. Figure 5 *c* and *d* further substantiates our interpretation of the phase plots. The data window over which KORRECT was performed was shifted forward in time, just as in the case of spectral analysis. As seen in the left panel of Figure 5, the strength of tidal periodicities steadily declines with time; by the end of the 12th day after the main shock, peaks at tidal periods vanish completely. Correspondingly, the phase variation curve of KORRECT for the semi-diurnal period exhibits a declining preference for the particular phases of the tidal cycle, and by the end of the 12th day, it loses its systematic character. This behaviour is shown in the right panel of Figure 5 for the 40 min pulse width.

From the combined results of the two independent analyses performed in this study, it is evident that the Earth tides had a strong influence on the occurrence times of aftershocks of the recent Tohoku-Oki earthquake. Two facts can be stated about the apparent weakening of the tidal-triggering effect with time. The first is that the steady decline in the number of aftershock makes it difficult to detect tidal periodicities. The second is that during the first few days after the main shock, there is very high level of activity due to which the focal mechanisms of many aftershocks would be favourable to triggering by tidal stresses. A word of caution regarding the faithfulness of the results obtained by KORRECT would be well-placed here. This method was originally developed to detect triggering of aftershocks by the free oscillations of the Earth. Free oscillations are normal modes wherein the entire Earth oscillates in phase. In case of the Earth tide, however, the induced variations are a function not only of time, but also of location. This fact is overlooked in the application of KORRECT for detection of tidal triggering. However, we still place faith in the use of this method because aftershocks of an earthquake occur over a limited geographical region over which the spatial variation of tidal oscillations can be neglected in a zeroth-order approximation[17]. KORRECT results clearly corroborate the presence of unambiguous peaks in the spectral analysis.

1. Scholz, C. H., *The Mechanics of Earthquakes and Faulting*, Cambridge University Press, New York, 1990, p. 470.

2. Vidale, J. E., Agnew, D. C., Johnston, M. J. S. and Oppenheimer, D. H., Absence of earthquake correlation with Earth tides: an indication of high preseismic fault stress rate. *J. Geophys. Res*., 1998, **103**, 24567–24572.
3. Tanaka, S., Ohtake, M. and Sato, H., Evidence for tidal triggering of earthquakes as revealed from statistical analysis of global data. *J. Geophys. Res*., 2002, **107**(B10), 2211; doi:10.1029/2001JB001577.
4. Knott, C. G., On lunar periodicities in earthquake frequency. *Proc. R. Soc. London*, 1896, **60**, 457–466.
5. Schuster, A., On lunar and solar periodicities of earthquakes. *Proc. R. Soc. London*, 1897, **61**, 455–465.
6. Emter, D., Tidal triggering of earthquakes and volcanic events. In *Tidal Phenomena, Lecture Notes in Earth Science* (eds Wilhelm, H., Zurn, W. and Wenzel, H.-G.), Springer-Verlag, New York, 1997, vol. 66, pp. 293–309.
7. Morgan, W. J., Stoner, J. O. and Dicke, R. H., Periodicity of earthquakes and the invariance of the gravitational constant. *J. Geophys. Res*., 1961, **66**, 3831–3843.
8. Tsuruoka, H., Ohtake, M. and Sato, H., Statistical test of the tidal triggering of earthquakes: contribution of the ocean tide loading effect. *Geophys. J. Int*., 1995, **122**, 183–194.
9. Shlien, S., Earthquake-tide correlation. *Geophys. J. R. Astron. Soc*., 1972, **28**, 27–34.
10. Shirley, J. H., Lunar and solar periodicities in large earthquakes: Southern California and the Alaska–Aleutian Islands seismic region. *Geophys. J*., 1988, **92**, 403–420.
11. Métivier, L., Viron, de O., Conrad, C., Renault, S., Diament, M. and Patau, G., Evidence of earthquake triggering by the solid earth tides. *Earth Planet. Sci. Lett*., 2009, **278**, 370–375.
12. Tanaka, S., Ohtake, M. and Sato, H., Tidal triggering of earthquakes in Japan related to the regional tectonic stress. *Earth Planets Space*, 2004, **56**, 511–515.
13. Kamal and Mansinha, L., The Triggering of aftershocks by the free oscillations of the earth. *Bull. Seismol. Soc. Am*., 1996, **86**, 299–305.
14. Ryall, A., VanWormer, J. D. and Jones, A. E., Triggering of microearthquakes by earth tides, and other features of the Truckee, California, earthquake sequence of September, 1966. *Bull. Seismol. Soc. Am*., 1968, **58**, 215–248.
15. Souriau, M., Souriau, A. and Gagnepain, J., Modeling and detecting interactions between Earth tides and earthquakes with application to an aftershock sequence in the Pyrenees. *Bull. Seismol. Soc. Am*., 1982, **72**, 165–180.
16. Heaton, T. H., Tidal triggering of earthquakes. *Geophys. J. R. Astron. Soc*., 1975, **43**, 307–326.
17. Hartmann, T. and Wenzel, H.-G., The HW95 tidal potential catalogue. *Geophys. Res. Lett*., 1995, **22**, 3553–3556.

ACKNOWLEDGEMENTS. We used the freely available NEIC earthquake catalogue data on the internet. We thank the anonymous reviewer for critical comments.

Received 24 May 2011; revised accepted 27 January 2012